Coordination Chemistry Reviews 254 (2010) 2267–2280

Contents lists available at ScienceDirect

Coordination Chemistry Reviews

journal homepage: www.elsevier.com/locate/ccr

Review

Signal processing with multicomponent systems based on metal complexes

Matteo Amelia, Lei Zou[1], Alberto Credi*

Dipartimento di Chimica "G. Ciamician", Università di Bologna, via Selmi 2, 40126 Bologna, Italy

Contents

ARTICLE INFO

Article history:
Received 30 October 2009
Accepted 3 January 2010
Available online 7 January 2010

In memory of Graziano Picco.

Keywords:
Electrochemistry
Logic gate
Memory
Nanoscience
Photochemistry
Supramolecular chemistry

ABSTRACT

Molecular-level systems that respond to external stimulation by changing some physical or chemical properties can be viewed as input–output devices and therefore may be useful for processing information. In recent years, several investigations on species capable of mimicking the function of macroscopic wires, switches, connectors, memories, logic gates, and circuits have been reported. The rational basis for this research stems from the fact that in living organisms information is transported, elaborated and stored by molecular or ionic substrates operating in a solution-based environment. Because of their diverse and valuable physico-chemical properties, metal complexes have been extensively used as functional components for the construction of artificial molecular devices capable of processing information. Here we illustrate recent progress, and discuss limitations and perspectives of this research area.

1. Introduction

1.1. *Signal processing in solid-state electronic devices*

In present day computers, data are elaborated electronically by microprocessor systems – that is, circuits based on bulk solid-state semiconductors which employ electrical input and output signals – and exchanged optically between remote locations. Computer circuits are made of a number of interconnected basic elements

---

* Corresponding author. Tel.: +39 051 2099540; fax: +39 051 2099456.
E-mail address: alberto.credi@unibo.it (A. Credi).

[1] Present address: Key Laboratory for Advanced Materials and Institute of Fine Chemicals, East China University of Science and Technology, Shanghai 200237, PR China.

0010-8545/$ – see front matter © 2010 Elsevier B.V. All rights reserved.
doi:10.1016/j.ccr.2010.01.001

(logic gates) that are mostly of the same type. Huge arrays of logic gates can be built up to achieve selected functions of varying complexity.

Data processing and communication require the encoding of information in electrical and optical signals in the form of binary digits (bits) [1]. This choice provides a robust "all or nothing" representation that ensures protection of data against noise accumulated in serial operations and originated from signal transduction and transmission. In order to digitally encode a (inherently analog) physical or chemical signal, a threshold value and a logic convention have to be established. In a positive logic convention, a 0 is used to represent a signal that is below the threshold voltage and a 1 is employed to indicate a signal that is above. In this frame, the logic circuits of microprocessor systems elaborate binary data through sequences of logic gates that operate according to the rules of George Boole's binary algebra [2].

It is worthwhile recalling that in communication networks, bundles of optical fibers can transmit hundreds of gigabits per second since propagating light beams of different wavelengths do not interfere [3,4]. The routes of the optical signals travelling through these networks are determined by optoelectronic devices that, at the receiving end of each optical fiber, convert the incident optical inputs into electrical signals. Then, the electrical signals are reconverted into optical outputs which are routed along another optical fiber. The noninteracting properties of optical signals, however, do not apply to electric signals since only one electric signal can be transported through a single electric wire. This means that the electronic portion of the optoelectronic devices cannot handle the immense parallelism potentially offered by optical signals. Strategies have to be developed to switch the propagating optical signals with optical, rather than electrical, stimulations [5].

1.2. Signal processing in biological systems

In biological systems, information is processed not by electron transport along wires but by movement of ions or molecules and by conformational changes of molecules [6,7]. Within cells, and also between cells, information is carried from place to place by the use of messenger molecules and relies on Brownian motion. At the scale of the cell, diffusive motion is remarkably fast: any two molecules within a micrometer-size cell meet each other every second [6]. Over large distances, however, this simple kind of chemical signaling would be too slow so that evolution has created a longer range communication and information processing system, the brain and nervous system. Its signaling mechanism is again quite different compared to that of electronic computers. In fact, although a nerve pulse manifests itself as a pulse of electrical potential, it is not the movement of electrons that is carrying the information, but ultimately the movement of ions through the membrane [7].

Another difference between silicon-based and biological information processing should be emphasized [7]. In an electronic computer, there is a clear distinction between hardware and software. Hardware is a physical entity, useless without the direction of software. By contrast, software is a transient and non-corporeal entity, but capable of animating the otherwise inert hardware to perform the desired task. In biological information processing systems, the basic elements of logics are well defined chemical entities and a clear distinction between hardware and software is impractical. For example, the genetic code, i.e., the "software" of an organism, is embodied in DNA molecules which are physical objects with very specific properties, and the "hardware" consists again of molecules, proteins that assemble to form the machines that carry out the functions of the organism. There are also molecules, like RNA, that can properly be considered as both the software and the hardware, because they can read and carry information from the DNA to the protein machines that create new molecules according to the specification of the genetic code, but can also act as machines themselves.

1.3. Chemical computing

Molecular-level information processing can potentially be used to develop "molecular computers" [8–11] featuring extremely small size, low power consumption and unprecedented performance [12]. The term molecular computer still sounds weird to most chemists in spite of the fact that the Pimentel report, some 20 years ago, was explicit and optimistic in this regard [13].

Clearly, the development of a computing machine based on molecules that can make current solid-state devices obsolete is a very ambitious objective even for basic research. While it is true that conventional scaling methods of the semiconductor industry face increasing technical and fundamental challenges as device features are pushed towards the deep sub-100-nm regime [11,14,15], recent progress in transistor technology will enable continued trends in downscaling and improvements in performance of logic complementary metal-oxide-semiconductor (CMOS) transistors until at least the middle of the next decade [15,16].

Nevertheless, advances in chemical synthesis have allowed the design and construction of supramolecular systems in which a discrete number of structurally integrated components can perform quite complex functions. Although the components of a "molecular processor" will not necessarily have to operate in ways analogous to those of microelectronic circuits, effort has been devoted to the design, synthesis and characterization of chemical systems that mimic the operation of semiconductor circuit components (wires, switches, memories, logic gates and logic circuits) [17–28]. Leaving aside futuristic speculations on chemical computers, systems of this kind could perform relatively simple computing tasks that cannot be accomplished with silicon-based devices [29,30]. Examples taken from recent research include the encoding [31] and networking [32,33] of microscopic objects, parallel chemical analyses in microfluidic systems [34], control of the function of biomolecules [35], screening of diagnostic markers [36], and intelligent drug delivery *in vitro* [37,38] and *in vivo* [39].

1.4. Scope of the review

The chemical approach to information processing described above is typically based on the modular design and construction of multicomponent species in which each molecular subunit plays a specific role. Metal complexes, owing to their diverse and valuable physico-chemical behaviour – in particular regarding the photochemical, photophysical and redox properties – constitute extremely versatile building blocks. In this review we will illustrate representative examples, taken from the recent literature, of multicomponent chemical systems which contain metal compounds or whose operation is based on metal ion complexation. Because of space reasons, we shall not discuss molecular wires and switches; the reader is referred to excellent reviews on these topics [17–19]. Rather, we will focus on systems performing more advanced functions such as multifunctional switches, logic gates and circuits, and memory devices. In most instances they operate in solution-based environments and are investigated at the ensemble level; however, we will also describe a few systems supported on solid surfaces. Perspectives and limitations of these kinds of devices will be critically discussed.

2. Multifunctional switches and memories

2.1. Mimicking electrical extension cables at the molecular level

Supramolecular species whose components are connected by means of noncovalent forces can be disassembled and re-assembled [40] by modulating the interactions that keep the components together, with the consequent possibility of switching energy- or electron-transfer processes. Two-component systems of this type are reminiscent of plug–socket electrical devices because, like their macroscopic counterparts, they are characterized by the possibility of reversibly connecting–disconnecting the two components, and the occurrence of a flow of electrons or electronic energy from the socket to the plug when the two components are connected. Molecular plug–socket systems of this kind have been reported [41–43].

The plug–socket concept, described above, can be used to design molecular systems which mimic the function played by a macroscopic electrical extension cable. The operation of an extension cable is more complex than that of a plug–socket system, because it involves *three* components that must be held together by *two* connections that have to be controllable *reversibly* and *independently*; in the fully connected system, an electron or energy flow must take place between the remote donor and acceptor units (Fig. 1).

In the attempt to construct a molecular-level extension cable for electron transfer, the pseudorotaxane, shown in Fig. 2a, made of the three components **1**$^{2+}$, **2**-H^{3+}, and **3**, was constructed and studied [44]. Component **1**$^{2+}$ consists of two moieties: a [Ru(bpy)$_3$]$^{2+}$ unit, which behaves as an electron donor when excited with light, and a dibenzo[24]crown-8 macrocycle, capable of playing the role of a hydrogen-bonding first socket. The dialkylammonium-based moiety of **2**-H^{3+}, driven by hydrogen-bonding interactions, threads as a plug into the first socket, whereas the π-electron accepting 4,4′-bipyridinium unit threads as a plug into the third component **3**, the π-electron rich 1,5-dinaphtho[38]crown-10 macrocycle, which plays the role of a second socket. In CH_2Cl_2:CH_3CN (98:2, v/v) solution, reversible connection–disconnection of the two plug–socket junctions, can be controlled independently by acid–base and redox stimulation, respectively, and monitored by changes in the absorption and emission spectra, owing to the different nature of the interactions (hydrogen-bonding and π-electron donor–acceptor) that connect the components. In the fully assembled triad, **1**$^{2+}\supset$**2**-H$^{3+}\subset$**3**, light excitation of the [Ru(bpy)$_3$]$^{2+}$ unit of the component **1**$^{2+}$ is followed by electron transfer to the bipyridinium unit of the component **2**-H^{3+}, which is plugged into component **3**.

In the system described above the transferred electron does not reach the final component of the assembly. Moreover, a true extension cable should contain a plug and a socket at the two ends, instead of two plugs as component **2**-H^{3+}. An improved system of that type has been recently investigated (Fig. 2b) [45]. The electron-source component is again **1**$^{2+}$, whereas the new extension cable **4**-H^{+} is made up [46] of a dialkylammonium ion, that can insert itself as a plug into a dibenzo[24]crown-8 socket, a biphenyl spacer, and a benzonaphtho[36]crown-10 unit, which fulfills the role of a π-electron rich socket. Finally, the 1,1′-dioctyl-4,4′-bipyridinium dication **5**$^{2+}$ can play the role of an electron drain plug. As for the previously studied system, the two plug–socket connections **1**$^{2+}\supset$**4**-H^{+} and **4**-H$^{+}\supset$**5**$^{2+}$ can be controlled by acid–base and redox stimuli, respectively.

In the complete ensemble, **1**$^{2+}\supset$**4**-H$^{+}\supset$**5**$^{2+}$, light excitation of the Ru-based unit of **1**$^{2+}$ is followed by electron transfer to **5**$^{2+}$, with **4**-H^{+} playing the role of an extension cable (Fig. 2b). The occurrence of this process is confirmed by nanosecond laser flash photolysis experiments, showing a transient absorption signal assigned to the 4,4′-bipyridinium radical cation formed by photoinduced electron transfer within the self-assembled triad. Such a second-generation system exhibits two conceptual and quite significant advancements: (i) **4**-H^{+} consists of a plug and a socket components, and thus it really mimics an extension cable; (ii) the photoinduced electron transfer does occur from the first component – the Ru-based unit of **1**$^{2+}$ – to the remote **5**$^{2+}$ moiety, whereas in the previous system the electron receiving bipyridinium unit was a component of the cable.

2.2. A set–reset memory device based on a copper rotaxane

Catenanes and rotaxanes based on Cu(I)–polypyridine complexes represent an important class of interlocked compounds [47] that have proven interesting as molecular switches and machines [17,48]. An example of such compounds is rotaxane **6**$^{+}$ (Fig. 3), composed of an axle containing a bidentate ligand and two bulky stopper groups, and a wheel containing a bidentate (1,10-

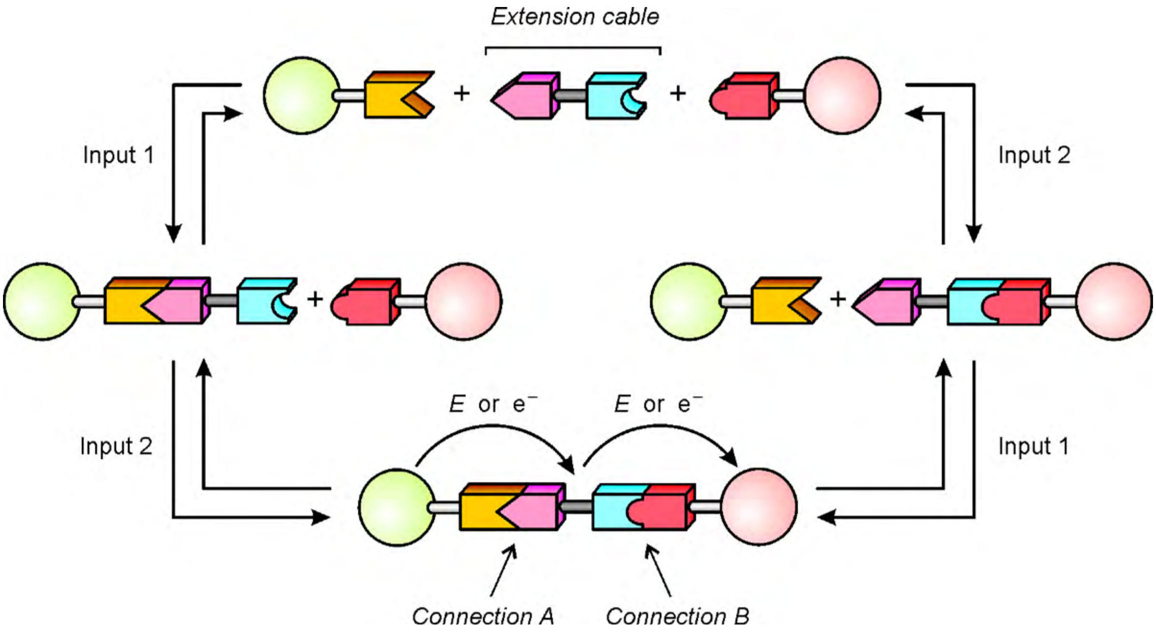

Fig. 1. Schematic representation of the working mechanism of an electrical extension cable.

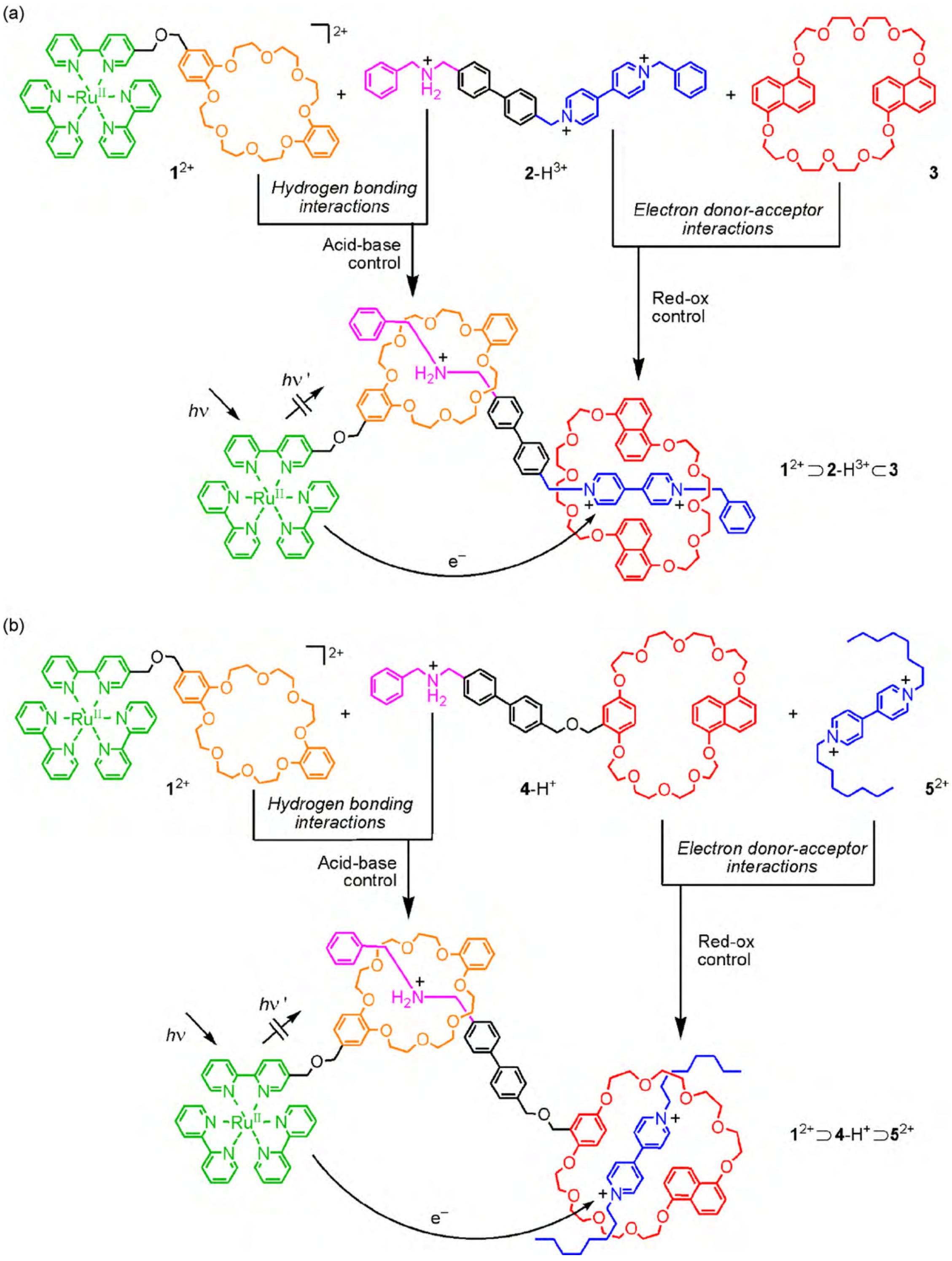

Fig. 2. First- and second-generation systems for mimicking an electrical extension cable. (a) Structural formulae of the three molecular components $\mathbf{1}^{2+}$, $\mathbf{2}$-H$^+$ and **3**, which self-assemble in solution to give the $\mathbf{1}^{2+}\supset\mathbf{2}\text{-H}^{3+}\subset\mathbf{3}$ triad. The photoinduced electron-transfer process from the Ru-based unit of $\mathbf{1}^{2+}$ to the bipyridinium unit of $\mathbf{2}$-H^{3+} taking place in the fully connected system is also represented [44]. (b) Structural formulae of the three molecular components $\mathbf{1}^{2+}$, $\mathbf{4}$-H$^+$ and $\mathbf{5}^{2+}$ which self-assemble in solution to give the $\mathbf{1}^{2+}\supset\mathbf{4}\text{-H}^{+}\supset\mathbf{5}^{2+}$ triad. In the fully connected system, excitation with visible light of the Ru-based unit of $\mathbf{1}^{2+}$ is followed by electron transfer to $\mathbf{5}^{2+}$, with $\mathbf{4}$-H$^+$ playing the role of an extension cable [45].

phenanthroline) and a tridentate (2,2′:6′,2″-terpyridine) ligands to which Cu$^+$ ions can bind [49]. The electrochemical oxidation of Cu(I) to Cu(II) results in the reorganization of the tetracoordinated complex $\mathbf{6}^{2+}$*(4)* into a pentacoordinated one, $\mathbf{6}^{2+}$*(5)*, via the pirouetting of the wheel around the axle. Cyclic voltammetric experiments showed that the process is reversible and were employed to determine the rotation rates (Fig. 3). The ability of rotaxane $\mathbf{6}^{+}$ to undergo reversible geometrical reorganization between the two different metal oxidation states makes it an attractive candidate for implementing a set–reset memory device [50].

A set–reset device is a finite-state machine which starts in an initial state and processes inputs one at a time; given the current

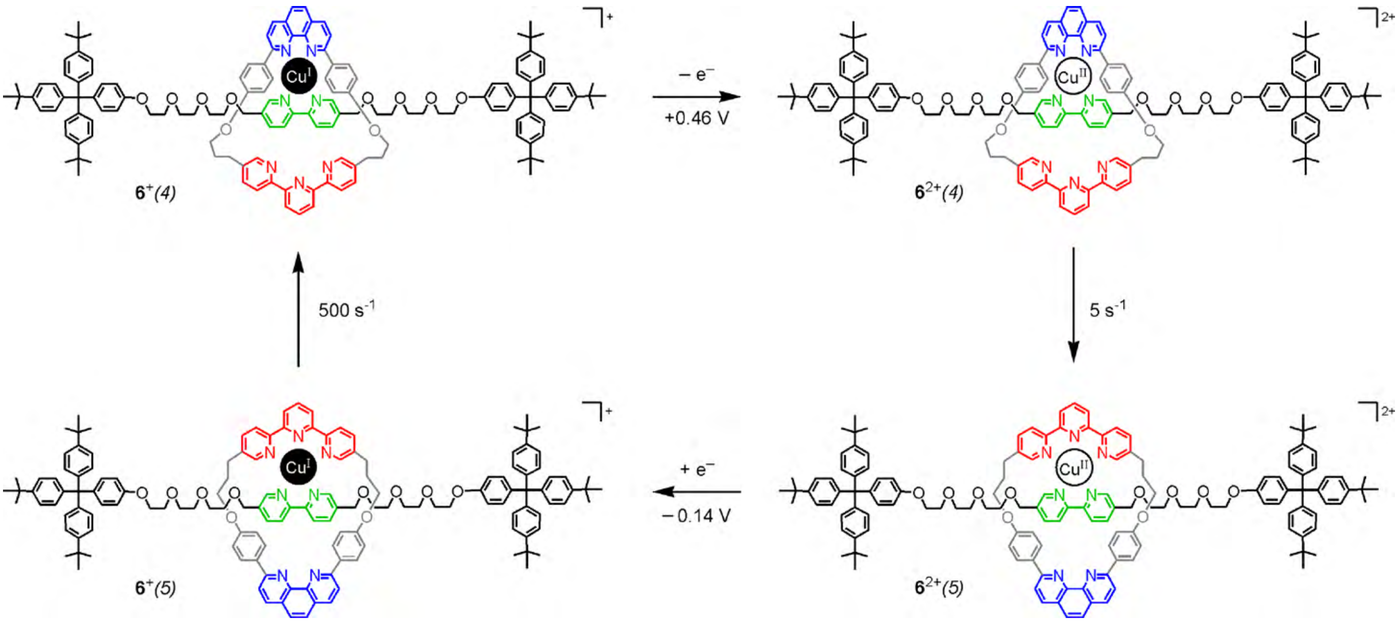

Fig. 3. The electrochemical switching of the redox states in the Cu rotaxane **6**$^{+}$ (horizontal reactions) is followed by ligand reorganization (vertical reactions) [49]. Peak potential values for the redox processes (in V versus an Ag quasi-reference electrode) and rate constants for the intramolecular rearrangements in acetonitrile at room temperature are reported.

state and input, the new state and output are determined by a transition scheme as depicted in Fig. 4. The two stable states, **6**$^{+}$*(4)* and **6**$^{2+}$*(5)*, are shown in squares and correspond to logic {0} and {1}, respectively.

An essential feature of the operation of this system is the hysteresis due to the nature of the reorganization of the coordination about the Cu ion following redox stimulation [51]. Such a phenomenon leads to a large difference between the potential values for oxidation and reduction of the copper ion (see Fig. 3), and enables one to distinguish the set and reset transitions [50]. The set–reset implementation requires three potential values to be defined: set, reset, and do-nothing. The set potential was taken as +1.0 V (versus an Ag quasi-reference electrode), a value at which **6**$^{2+}$*(5)* is the stable species. Conversely, the reset potential was fixed at −0.4 V, a value at which the stable species is **6**$^{+}$*(4)*. The do-nothing potential has to be taken in the region of bistability; e.g., at +0.2 V the device is in state {0} [**6**$^{+}$*(4)*] for the oxidation process and in state {1} [**6**$^{2+}$*(5)*] for the reduction process. As shown in Fig. 4, application of a set input (+1.0 V) switches the device from state {0} to {1}; however, if the device is already in state {1} the set input has no effect. Application of a reset input (−0.40 V) switches the device from state {1} to {0} but has no effect if the device is already in state {0}. The do-nothing potential (+0.2 V) does not change the state irrespective of whether it is {0} or {1}. The state of the device can be read by monitoring the voltammetric current in response to the applied potential input, or by spectroscopic measurements. Clearly, this system operates as a memory because an information bit can be written by applying a set potential and remains memorized even when the writing potential is removed. The written data can be erased by applying a reset potential pulse. Owing to its chemical reversibility, the device can be cycled a large number of times.

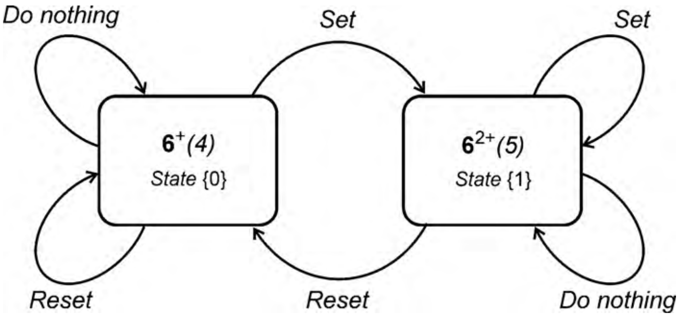

Fig. 4. Operation of a set–reset device based on the electrochemical switching and ligand reorganization processes represented in Fig. 3 for rotaxane **6**$^{+}$ [50]. See text for details.

3. Molecular logic gates and circuits

Logic gates are devices that perform Boolean operations on one or more inputs to produce an output [2]. Logic circuits can be viewed as network of basic logic gates that implement a more complex Boolean function. Each type of logic gate or circuit possesses a specific input–output signal correlation pattern described in the so-called truth table, which lists all the possible combinations of input–output states.

The first proposal to execute logic operations at the molecular level was made in 1988 [52], but the field developed only 5 years later when the analogy between molecular switches and logic gates was experimentally demonstrated [53]. In fact, as molecular switches convert input stimulations into output signals [17], the principles of binary (Boolean) logic can be applied to the signal transduction operated by molecules under appropriate conditions [54]. Following this approach, the most common Boolean functions (PASS, YES, NOT, AND, NAND, OR, NOR, XOR, XNOR, INH) have been implemented with chemical systems [18–27].

A critical issue of molecular logic gates is the interconnection of basic elements to create complex circuits [55,56], which is a key feature of electronic logic gates owing to their full input/output homogeneity. The construction of molecular logic networks, however, can take advantage of functional integration that can be achieved within one molecule by rational chemical design, rather than relying on intensive physical connection of elementary gates [29,57]. The fact that unsophisticated dye molecules in solution can perform complex logic functions [58–60] which, in silicon-based

(a)

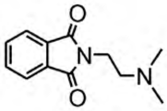

7

(b)

In$_1$ (O_2)	In$_2$ (Et_3N)	Out (544 nm)^a
0	0	1
0	1	0
1	0	0
1	1	0

^{a} Phosphorescence

(c)

In$_1$ (O_2)	In$_2$ (Cl^-)	Out (544 nm)^a
0	0	0
0	1	1
1	0	0
1	1	0

^{a} Phosphorescence

Fig. 5. Structural formula of phthalimide derivative **7** (a) and truth table for operation of its Tb^{3+} complexes as NOR (b) and INH (c) gates [63].

systems, require circuits made of several interconnected gates is a demonstration of this idea.

Such a high functional integration is possible owing to an important feature of molecular logic gates and circuits, namely reconfigurability [18,24–26,61]. This property refers to the possibility of defining different logic operations for the same gate. In silicon-based circuits reconfiguration of the logic operation is carried out by interrupting selected connections in gate arrays, usually in an irreversible manner [62]. Molecular logic systems can be reconfigured by changing the type of input/output signals or by using a separate switching stimulus. For instance, the logic expression for molecular logic gates with optical output signals and significant input-induced spectral shifts can be conveniently reconfigured by monitoring the output at a different wavelength.

In wavelength-reconfigurable logic gates different logic types are observed depending on the wavelength at which the output signal is monitored. Because multiple wavelength can be observed at the same time, such gates perform simultaneously different logic functions on a given set of inputs, a property that has been referred to as superposition or multiplicity of logic types [18,24–26,61]. Because logic superposition is a consequence of the multichannel nature of light, it does not occur with electronic systems.

These concepts will be better illustrated on the basis of the following recent examples, which in our opinion constitute prominent advances in the field of molecular logic.

3.1. Logic functions based on lanthanide luminescence

Compound **7** (Fig. 5a) forms 1:1, 2:1 and 3:1 complexes with Tb^{3+} ions in acetonitrile, in which the phthalimide chromophore sensitizes the lanthanide luminescence [63]. In this system the input signals are represented by specific chemical reactants (chloride ions, oxygen and triethylamine), whereas the output signal is coded for by the Tb^{3+} emission. The addition of either O_2 or triethylamine to a 1:1 mixture of **7** and Tb(III) triflate causes a decrease in the luminescence output because they both act as quenchers towards the triplet excited state of the phthalimide antenna chromophore. Hence, the output is high (state {1}) only if none of the inputs is applied, thus realizing a NOR operation (Fig. 5b).

The combination of O_2 and Cl^- as the chemical inputs led to an output response characteristic of an inhibit (INH) gate (Fig. 5c). In fact, chloride ions enhance dramatically the lanthanide luminescence, most likely because they bind to the Tb^{3+} ion and cause the removal of residual water or solvent molecules from the coordination sphere, thereby diminishing quenching by OH or CH oscillators. A strong phthalimide-sensitized Tb^{3+} luminescence was observed in the absence of oxygen and in the presence of Cl^-, while all other combinations of these two inputs led to much weaker signals.

Since chloride ions increase strongly the lanthanide luminescence, they can be used to switch on and off the output of the NOR gate described above (Fig. 5b). As a result, the NOR gate that operates on oxygen and triethylamine inputs is open only when Cl^- ions are supplied, giving rise to a three-input enabled NOR (EnNOR) function.

3.2. 'Plug and play' molecular logic via self-assembly in micelles

The concept of 'plug and play' is of particular convenience for electronic devices because the addition of new modules directly enables new functions. This concept was very recently demonstrated for molecular logic devices by arranging the association between easily available luminophores and receptors in micelles (Fig. 6) [64].

An aqueous solution of the neutral surfactant Triton X-100 above its critical micellar concentration, when interrogated with 450-nm excitation and 625 nm observation, shows no emission with either 'high' or 'low' H^+ concentration as the input, because it lacks a suitable chromophore. This simple behaviour corresponds to a PASS 0 function driven by a proton input, i.e., the output is always 0 irrespective of the input state (Fig. 6a). Addition of the hydrophobic $[Ru(bpy)_3]^{2+}$-type complex $\mathbf{8}^{2+}$ (Fig. 7) enables the luminophore to reside within the micelles. Interrogation as before produces a 'high' emission signal irrespective of the proton concentration, because there are no basic sites to engage H^+, thus emulating PASS 1 logic (Fig. 6b).

Further addition of receptor $\mathbf{9}^{2-}$ (Fig. 7) allows most of the micelles occupied by $\mathbf{8}^{2+}$ to co-include $\mathbf{9}^{2-}$. Interrogation as before at pH 12 gives a 'low' luminescence output because of intra-micellar photoinduced electron transfer from the aromatic amine to the ruthenium complex. In contrast, the emission output is enhanced by almost one order of magnitude at pH 2, because the quenching effect of the amine is prevented by its protonation. Hence, the emission output reproduces the H^+ input, corresponding to YES logic (Fig. 6c). As $\mathbf{9}^{2-}$ is also a receptor for Ca^{2+} ions, the micelle system containing $\mathbf{8}^{2+}$ and $\mathbf{9}^{2-}$ can be subjected to both H^+ and Ca^{2+} inputs. In such a case, a 'high' output is observed in all cases except when both inputs are 'low', realizing OR logic (Fig. 6d).

t-Butylphenolate $\mathbf{10}^{-}$ (Fig. 7) can also be profitably used as pH-switchable quencher for $\mathbf{8}^{2+}$, affecting the luminescence of the latter in a qualitatively similar manner compared to $\mathbf{9}^{2-}$. However, the substantially different pK_a values of the conjugated acids of $\mathbf{9}^{2-}$ and $\mathbf{10}^{-}$ (5.8 and 9.9, respectively, in the examined conditions) enable to identify a pH range (8–12) in which the former loses its pH sensitivity and only responds to Ca^{2+}. Under these conditions, these two species behave as selective receptors for Ca^{2+} and H^+, respectively. If appropriate thresholds are used, the observation of emission at 625 nm upon 425-nm excitation for micelles containing $\mathbf{8}^{2+}$ and the two receptors gives a 'high' value only when both H^+

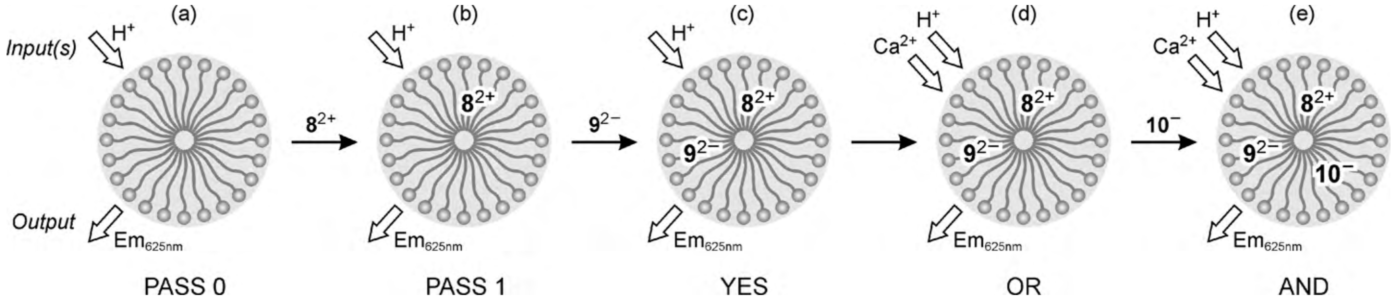

Fig. 6. Schematic representation of Triton X-100 micelles loaded according to a sequential addition of suitable luminophores and receptors (structures shown in Fig. 7). The micelle assemblies are subjected to H^+ and Ca^{2+} inputs; the observed output is emission at 625 nm upon excitation at 450 nm [64].

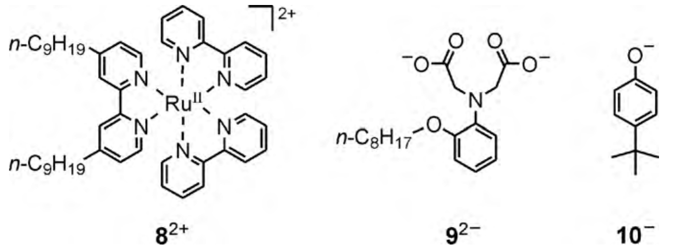

Fig. 7. Structure formulae of the luminophore and receptor molecules employed for the assembly of the responsive micelles shown in Fig. 6.

and Ca^{2+} inputs are applied, corresponding to AND logic (Fig. 6e). This is because the independent quenching action of the two receptors towards $\mathbf{8}^{2+}$ is disabled only if they are both occupied by the respective ionic input.

The main advantages of this approach based on self-assembly and input reconfiguration are its versatility and its very limited requirements in terms of synthetic effort.

3.3. All-optical logic gates based on signal communication between molecular switches

In most molecular logic gates, the input and output signals have a different physical nature; typically, they operate on ionic or molecular inputs and provide a photonic output, as described in the two previous sections. This input/output inhomogeneity is a severe problem if complex circuits are to be created because it prevents the interconnection of basic elements [55,56]. In contrast, serial connection of logic gates, also termed *cascading* – namely, the output of an upstream gate is sent as the input for a downstream gate – is extensively used in semiconductor circuits [1]. Molecular logic devices that use optical input and output signals [23,65–67] are particularly interesting in this regard, and also because (i) access for chemicals or wires is not required, (ii) no waste products are formed on repeated cycling of the device, (iii) operation in rigid or semirigid media is possible, and (iv) the multichannel nature of light can be exploited to configure the device for different logic functions. Prototypical examples of this type of molecular logic gates based on the control of porphyrin fluores-

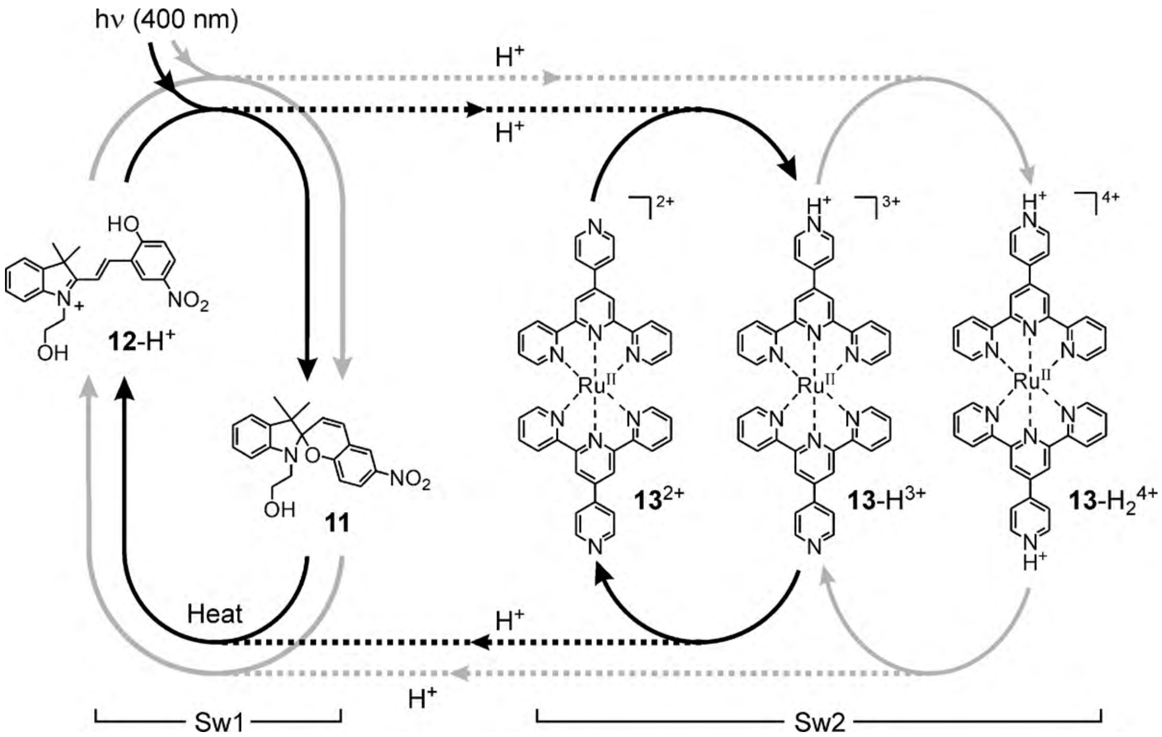

Fig. 8. Coupled operation of the two-state switch Sw1, based on the **11**/**12**-H^+ photochromic system, and three-state switch Sw2, based on the pH-sensitive Ru complex $\mathbf{13}^{2+}$, by means of light-induced proton exchange in acetonitrile at room temperature [68]. Irradiation of **12**-H^+ such that one equivalent of protons is transferred to the metal complex generates the **13**-$H_3{}^{3+}$ state (black lines). Further irradiation of **12**-H^+ can cause the transfer of another equivalent of protons to the metal complex, thereby obtaining the **13**-$H_2{}^{4+}$ state (grey lines). Subsequent thermal equilibration in the dark regenerates the starting state by reverse proton exchange.

cence by covalently linked photochromic units have been reported [23].

A different approach to devise all-optical molecular logic systems was recently reported [68]. This strategy is based on the coupled operation of two molecular switches, namely (i) a photoacid which transduces optical inputs into ionic outputs (Sw1), and (ii) a switch which responds to ionic inputs and provides optical outputs (Sw2). The two switching units communicate with one another by chemical signals and are connected serially, that is, the photogenerated ionic output of Sw1 is the input of Sw2. The concept was realized with the system shown in Fig. 8. Sw1 is based on a colorless spiropyran derivative, **11**, which is converted into the yellow protonated merocyanine form **12**-H^{+} in acid solution [69]. On irradiation with light of 400 nm, **12**-H^{+} isomerizes back to **11** and releases a proton into the solution. Sw2 is **13**$^{2+}$, a $[\mathrm{Ru(tpy)_2}]^{2+}$ complex (tpy = 2,2′:6′,2″-terpyridine) complex having 4-pyridyl substituents in the 4′-position of each tpy ligand. In solution, this complex can exist in three different protonation states, namely, **13**$^{2+}$, **13**-H^{3+} and **13**-H$_2$$^{4+}$. Spectroscopic titrations showed that these three forms: (i) exhibit distinct and characteristic absorption spectra, and luminescence spectra and lifetimes, (ii) they can be populated selectively, because the two pendant pyridyl units of **13**$^{2+}$ can be sequentially protonated in two consecutive steps, and (iii) they are reversibly interconverted by stoichiometric additions of acid and base [70]. Therefore, **13**$^{2+}$ behaves as an acid–base controlled three-state luminescent switch. As **11** and **12**-H^{+} exhibit smaller and larger pK_a values than that of the pyridinium ion, respectively [71], the protonation state of the ruthenium complex could be controlled by light, using **11**-H^{+} as a photoacid.

As shown in Fig. 8, irradiation of **12**-H^{+} at 400 nm in acetonitrile such that one equivalent of protons is transferred to the metal complex generates the **13**-H^{3+} state. Further irradiation of **12**-H^{+} can cause the transfer of another equivalent of protons to the metal complex, thereby generating the **13**-H$_2$$^{4+}$ state. Subsequent thermal equilibration in the dark regenerates the initial state by reverse proton exchange. Several irradiation/thermal equilibration cycles can be repeated on the same solution without appreciable degradation of the components.

The analysis of the behaviour of this system in terms of binary logic shows that all-optical two-input AND, OR and XNOR functions are obtained (Fig. 9). Both inputs are coded for by irradiation with 400-nm light. The input string {0,0} corresponds to dark conditions, whereas the input strings {1,0} and {0,1} correspond to irradiation with the amount of 400-nm light needed to transfer one equivalent of protons from **12**-H^{+} to **13**$^{2+}$ so that the complex **13**-H^{3+} is formed. The molecular system cannot distinguish between these input strings but the operator does, because the two light inputs can be supplied by two physically independent channels. The input string {1,1} corresponds to irradiation with a dose of 400 nm photons such that two equivalents of protons are transferred from **12**-H^{+} and the complex **13**-H$_2$$^{4+}$ is obtained. The optical output is represented by the luminescence intensity of the metal complex upon excitation at 493 nm. If the emission is monitored at 732 nm, application of an appropriate threshold enables emulation of the AND operation; the OR function can also be obtained by applying a different threshold (Fig. 9). The XNOR function can be performed by reconfiguring the monitored emission wavelength to 626 nm. The same approach was employed to control the luminescence of the Os(II) analog of **13**$^{2+}$ and the photoinduced generation of singlet oxygen [72].

3.4. Ruthenium tris(bipyridine) as a prototype of encoder/decoder

Digital encoders and decoders are combinational circuits, i.e., circuits in which the output values are determined solely by the current value of the inputs [2]. Combinational circuits are networks of basic logic gates that implement Boolean logic functions and can be described by a truth table. The function performed by a digital encoder is that of converting data into a code, an operation that is useful to compress information that have to be transmitted or stored. A 4-to-2 encoder, for example, compresses four inputs into two output channels (Fig. 10a). Conversely, a 2-to-4 decoder converts two coded inputs into four readable outputs (Fig. 10b). Molecular systems that emulate the function of an encoder or a decoder have been reported [73,74].

(a)

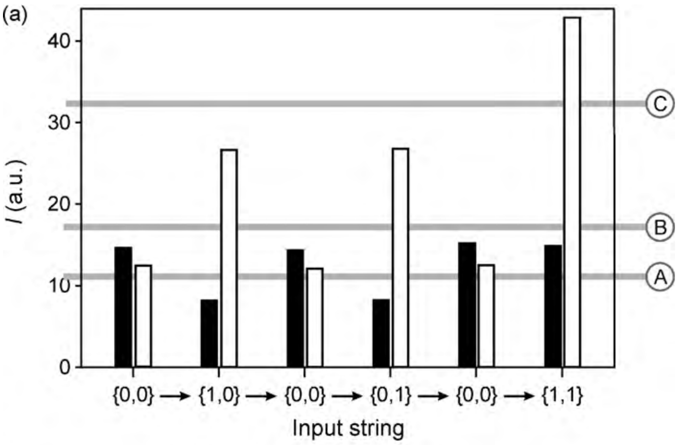

(b)

In$_1$ (400 nm)^a	In$_2$ (400 nm)^a	Out$_1$ (626 nm)^b Threshold A	Out$_2$ (732 nm)^b Threshold B	Threshold C
0	0	1	0	0
0	1	0	1	0
1	0	0	1	0
1	1	1	1	1
		⇩ XNOR	⇩ OR	⇩ AND

^{a} Irradiation ^{b} Luminescence

Fig. 9. (a) Response of the ensemble schematized in Fig. 8 to different input strings and cycling. Filled and empty bars represent the experimental luminescence intensity at 626 nm (Out$_1$) and 732 nm (Out$_2$), respectively (λ_{exc} = 493 nm). Marks A, B and C represent the threshold values for the XNOR, OR and AND operations, respectively. Input conditions: {0,0}, 10 h at 318 K; {1,0} and {0,1}, irradiation at 400 nm for 15 min; {1,1}, exhaustive irradiation at 400 nm.

It was shown very recently that simple $[\mathrm{Ru(bpy)_3}]^{2+}$ hexafluorophosphate in acetonitrile can mimic the operation of both a 4-to-2 encoder and a 2-to-4 decoder operations [60]. These functions are obtained thanks to the unique physico-chemical properties of this complex [75], and in particular the possibility of: (i) absorbing visible light; (ii) forming a long lived and luminescent triplet excited state, $^*[\mathrm{Ru(bpy)_3}]^{2+}$, by light irradiation; (iii) undergoing reversible monoelectronic oxidation and reduction processes to yield $[\mathrm{Ru(bpy)_3}]^{3+}$ and $[\mathrm{Ru(bpy)_3}]^{+}$, respectively, characterized by distinct absorption spectra, and; (iv) generating the triplet excited state via the comproportionation reaction between the oxidized $[\mathrm{Ru(bpy)_3}]^{3+}$ and the reduced $[\mathrm{Ru(bpy)_3}]^{3+}$ species [76], thereby enabling electrochemiluminescence generation (Fig. 11). The starting state is $[\mathrm{Ru(bpy)_3}]^{2+}$; the system is reset to this state (if required, by application of a potential value of 0 V) prior to each input operation.

For the encoder function (Fig. 10a) the four inputs are, respectively, oxidation at +1.4 V versus the SCE (In$_1$), low-power

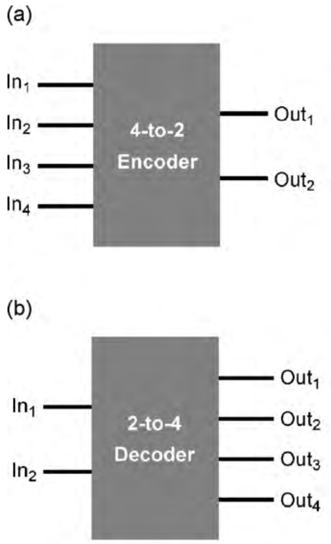

(a)

In$_1$ (+1.4 V)^a	In$_2$ (450 nm)^b	In$_3$ (−1.4 V)^c	In$_4$ (+1.4/−1.4 V)^d	Out$_1$ (530 nm)^e	Out$_2$ (620 nm)^f
1	0	0	0	0	0
0	1	0	0	0	1
0	0	1	0	1	0
0	0	0	1	1	1

^{a} Oxidation ^{b} Excitation ^{c} Reduction ^{d} Alternating oxidation/reduction ^{e} Absorption ^{f} Luminescence

(b)

In$_1$ (+1.4 V)^a	In$_2$ (−1.4 V)^b	Out$_1$ (450 nm)^c	Out$_2$ (310 nm)^c	Out$_3$ (530 nm)^c	Out$_4$ (620 nm)^d
0	0	1	0	0	0
1	0	0	1	0	0
0	1	0	0	1	0
1	1	0	0	0	1

^{a} Oxidation ^{b} Reduction ^{c} Absorption ^{d} Luminescence

Fig. 10. Schematic representation (left) and truth table (right) of a 4-to-2 encoder (a) and a 2-to-4 decoder based on $[Ru(bpy)_3]^{2+}$ [60]. See text for details.

excitation at 450 nm (In_2), reduction at −1.4 V (In_3) and alternating oxidation/reduction by a square wave potential oscillating between +1.4 and −1.4 V (In_4). The two outputs are coded for by the absorbance at 530 nm (Out_1) and the luminescence intensity at 620 nm (Out_2), respectively. Application of In_1 (+1.4 V) converts $[Ru(bpy)_3]^{2+}$ into $[Ru(bpy)_3]^{3+}$, which exhibits neither absorption at 530 nm ($Out_1 = \{0\}$) nor emission at 620 nm ($Out_2 = \{0\}$). In_2, which involves low-power excitation of $[Ru(bpy)_3]^{2+}$ at 450 nm, causes no change in absorbance ($Out_1 = \{0\}$) and produces 620-nm luminescence ($Out_2 = \{1\}$). Application of In_3 (−1.4 V) converts $[Ru(bpy)_3]^{2+}$ into $[Ru(bpy)_3]^{+}$, which absorbs at 530 nm ($Out_1 = \{1\}$) and does not emit ($Out_2 = \{0\}$). Finally, application of In_3 (alternating +1.4 and −1.4 V) leads to an electrostationary state containing $[Ru(bpy)_3]^{2+}$, $[Ru(bpy)_3]^{3+}$, $[Ru(bpy)_3]^{+}$, and $^*[Ru(bpy)_3]^{2+}$. Upon optimization of the experimental conditions, an absorption at 530 nm higher than the fixed threshold ($Out_1 = \{1\}$) and emission at 620 nm ($Out_1 = \{1\}$) can be obtained.

For the 2-to-4 decoder function (Fig. 10b) the two inputs are oxidation at +1.4 V (In_1) and reduction at −1.4 V (In_2); the outputs are coded for, by the absorbance at 450 nm (Out_1), 310 nm (Out_2), 530 nm (Out_3) and the emission at 620 nm (Out_4). If no input is applied (In_1 and $In_2 = \{0\}$), the solution exhibits the absorption band of at 450 nm ($Out_1 = \{1\}$), while all other output channels are in state $\{0\}$. Activation of In_1 (+1.4 V) converts $[Ru(bpy)_3]^{2+}$

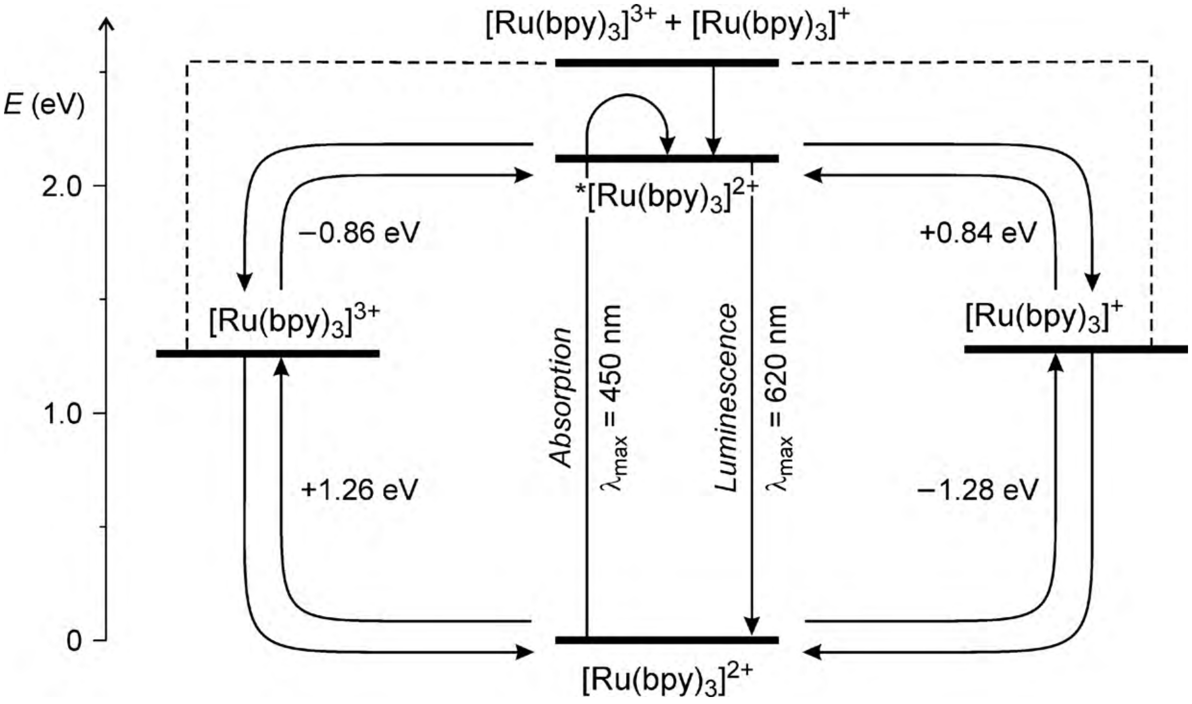

Fig. 11. Simplified energy diagram illustrating the main spectroscopic and redox processes for $[Ru(bpy)_3]^{2+}$ [75]. The energy levels of the oxidized and reduced species are obtained from the redox potential values referred to the SCE electrode. The diagram also shows that the reaction between the one-electron oxidized and reduced forms of this species is sufficiently exoergonic to generate luminescence [76].

into $[\mathrm{Ru(bpy)_3}]^{3+}$, which shows substantial absorption at 310 nm ($\mathrm{Out_2} = \{1\}$) and neither absorption at 450 and 530 nm or emission at 620 nm ($\mathrm{Out_1}$, $\mathrm{Out_3}$ and $\mathrm{Out_4} = \{0\}$). Application of $\mathrm{In_2}$ (−1.4 V) generates $[\mathrm{Ru(bpy)_3}]^{+}$, which has an absorbance higher than the threshold at 530 nm ($\mathrm{Out_3} = \{1\}$), but lower than the threshold at 450 and 310 nm, and no emission at 620 nm ($\mathrm{Out_1}$, $\mathrm{Out_2}$ and $\mathrm{Out_4} = \{0\}$). Finally, concomitant oxidation at +1.4 V and reduction at −1.4 V of $[\mathrm{Ru(bpy)_3}]^{2+}$ with a bipotentiostat ($\mathrm{In_1}$ and $\mathrm{In_2} = \{1\}$) produces an electrostationary state that contains $[\mathrm{Ru(bpy)_3}]^{2+}$, $[\mathrm{Ru(bpy)_3}]^{3+}$, $[\mathrm{Ru(bpy)_3}]^{+}$, and $^{*}[\mathrm{Ru(bpy)_3}]^{2+}$. Again, by adjusting the experimental conditions, absorbance values at 450, 310 and 530 nm below the respective threshold can be obtained ($\mathrm{Out_1}$, $\mathrm{Out_2}$ and $\mathrm{Out_3} = \{0\}$), together with an emission at 620 nm which is continuously produced by annihilation of the electrogenerated $[\mathrm{Ru(bpy)_3}]^{3+}$, $[\mathrm{Ru(bpy)_3}]^{+}$ species ($\mathrm{Out_4} = \{1\}$).

This logic system is based on an unsophisticated molecule, it is reconfigurable in situ without the addition of chemical reagents, and it can be cycled without formation of waste products.

3.5. A molecular keypad lock

In contrast with combinational circuits, whose outputs are determined only by the current state of the inputs, sequential circuits are logic networks whose output depends on both the *current* and *past* values of the inputs [2]. In other words, whereas combinational circuits like adder, subtractor, multiplexer/demultiplexer and encoder/decoder combine the current input states, in some way, to produce the output and hence have no memory, sequential circuits use the sequence of the input states over time to determine the output. In fact, memory circuits are inherently sequential (see Section 2.2). In logic design sequentiality is achieved by introducing feedback loops, that is, the output of a certain logic gate is sent back as one of its inputs or as the input of another upstream gate. This feedback mechanism disrupts the unidirectional information flow that is a fundamental characteristic of combinational circuits. Under a chemical point of view the time variable is put into the game by exploiting the different rates of the processes involved in the gate operation. In chemical terms one could say

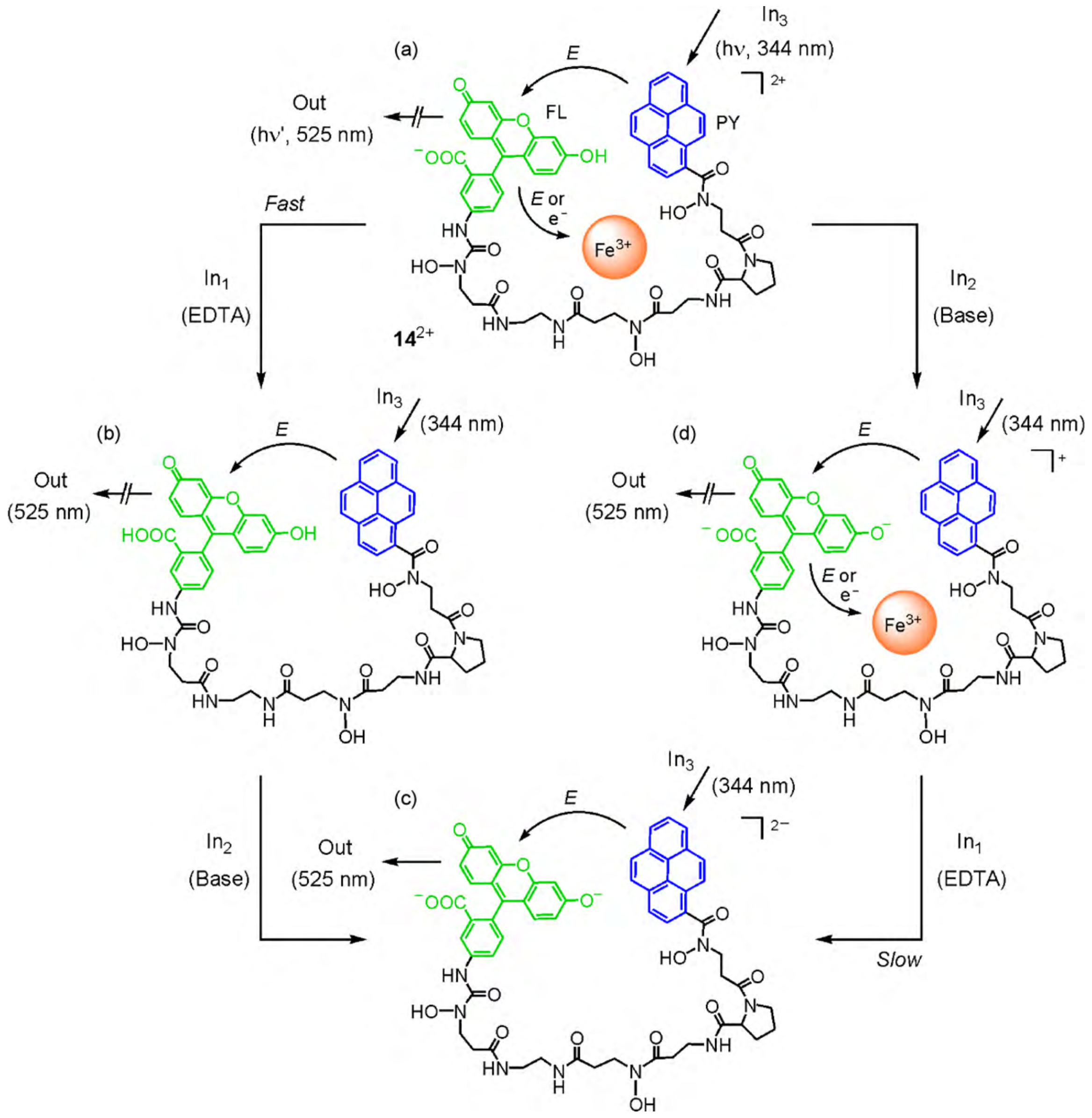

Fig. 12. Structure formula of the Fe(III) complex $\mathbf{14}^{2+}$ (a) and chemical transformations induced by the addition of EDTA (b), base (d), and both (c). This molecular device can recognize the correct sequence of three input signals (EDTA, base, 344-nm excitation) [81].

that combinational logic can be achieved with molecules by relying on equilibrium states, whereas sequential logic requires also the analysis (and possibly optimization) of the kinetic behaviour of the system.

Examples of chemical systems whose properties are interpreted in terms of sequential logic operation have started to appear only in the past few years [77–80]. An important step in this direction is represented by the investigation on a molecular species in solution whose fluorescence is switched on only in response to a correct sequence of three input signals [81]. Such a system is reminiscent of an electronic keypad lock, a common security device that can control the opening of a door or a safe. The molecular keypad lock is based on the Fe(III) complex **14**$^{2+}$ (Fig. 12a), which comprises fluorescein (FL) and pyrene (PY) fluorophores connected by a linker which is also a ligand (siderophore) capable of binding ferric ions strongly and selectively [82]. In ethanol compound **14**$^{2+}$ contains the fluorescein moiety in its monoanionic form and most likely exhibits a folded structure in which the FL and PY moieties can approach each other. The inputs are coded for by a chelating agent for Fe(III) (EDTA, In$_1$), a basic reactant (sodium acetate, In$_2$), and UV irradiation (In$_3$), whereas the output channel is identified as the fluorescein emission at 525 nm.

In the starting state the emission of the FL anion moiety is quenched by the metal ion (Fig. 12a). Addition of EDTA extracts the iron ion from the siderophore but also protonates the FL unit, transforming it to the non-emissive neutral state (Fig. 12b). Subsequent addition of acetate ions leads to the formation of the FL dianion, which is strongly fluorescent (Fig. 12c). Alternatively, addition of acetate ions to **14**$^{2+}$ causes the formation of the FL dianion, whose fluorescence is quenched by the still bound metal ion (Fig. 12d). It is clear that inverting the order of the inputs (first base, then EDTA) leads ultimately to the same state, resulting in strong emission at 525 nm (Fig. 12c). However, as the extraction of a ferric ion from a siderophore by EDTA is inhibited in a basic environment, a substantial difference in the reaction rate between the two paths ($a \rightarrow b \rightarrow c$ and $a \rightarrow d \rightarrow c$) is observed. On the other hand, no photoluminescence can be monitored without light excitation: this provides the basis for the third input signal, namely, irradiation at 344 nm. Light of this wavelength is mainly absorbed by the PY unit, which then sensitizes the FL luminescence by energy transfer. Therefore, by reading the response of the device not later than a few minutes after activation of the inputs, fluorescence at 525 nm is observed only if the correct sequence In$_1$ (EDTA), In$_2$ (base), In$_3$ (UV excitation) is supplied. Any other inputs combination leads to weak or no fluorescence. In other words, activation of In$_3$ generates an output only if the current state of In$_1$ and In$_2$ is $\{1,1\}$ and the previous state was $\{1,0\}$, showing the sequential behaviour of the system.

3.6. Molecular logic devices on surfaces

While molecule-based logic systems in solution are useful for proof-of-principle studies and for some applications (e.g., sensing), they are impractical for integration into real devices that can be addressed through an external interface [18]. Moreover, compatibility with microelectronic circuits would be required, in order to develop a hybrid technology that would constitute a viable alternative to continue pushing the top-down fabrication techniques towards their physical limits [11]. In such a context the development of molecule-based logic gates that function in heterogeneous environments, e.g., on surfaces or at interfaces, is an important task [83].

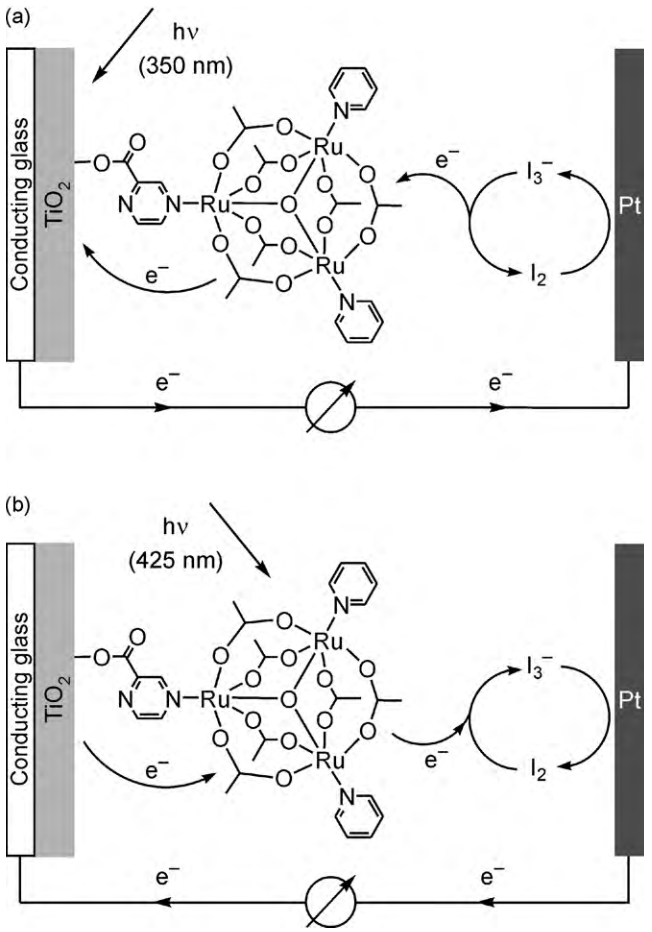

Fig. 13. Scheme of a photoelectrochemical cell based on a Ru cluster bound to a TiO_2 nanostructured electrode. The system behaves as an XOR hate with optical inputs and electric current output [88].

A first step in this direction is represented by the construction of suitably functionalized electrodes and the analysis of their behaviour in terms of Boolean logic. For example, electrodes derivatized with chemical compounds are extensively used in solar cells, display devices and switching applications, but their potential as logic systems has been recognized only recently [84–89].

A logic gate based on a ruthenium cluster adsorbed on the surface of a TiO_2 nanocrystalline electrode of a photoelectrochemical solar cell is schematized in Fig. 13 [88]. Differently from what is desired for photovoltaic applications, the metal complex is designed such that its excited state is reductively quenched by the semiconductor. In this system, TiO_2 bandgap excitation (e.g., $\lambda = 350$ nm) causes the appearance of an anodic current, as normally observed for bare titanium dioxide electrodes (Fig. 13a). However, irradiation with 425-nm light results in excitation of the metal cluster and formation of an excited state, that can accept an electron from the TiO_2 valence band. The reduced cluster subsequently transfers an electron to the redox mediator (I_2) and a cathodic current is observed (Fig. 13b). These properties can be exploited to carry out logic operations. Irradiation with light of either 350 or 425 nm (inputs) results in a net photocurrent output. However, upon simultaneous irradiation at both wavelengths cathodic and anodic current components cancel out and no current output is observed. Hence, XOR logic is demonstrated [85]. A relevant feature of this system is the transduction of the optical inputs into an electrical output. A related study demonstrated logic reconfiguration of the gate by applying a potential to the electrode [87].

In another interesting series of investigations, monolayers of $[Os(bpy)_3]^{2+}$ and $[Ru(bpy)_3]^{2+}$-type complexes on glass substrates were constructed and investigated (Fig. 14) [90–92]. These metal

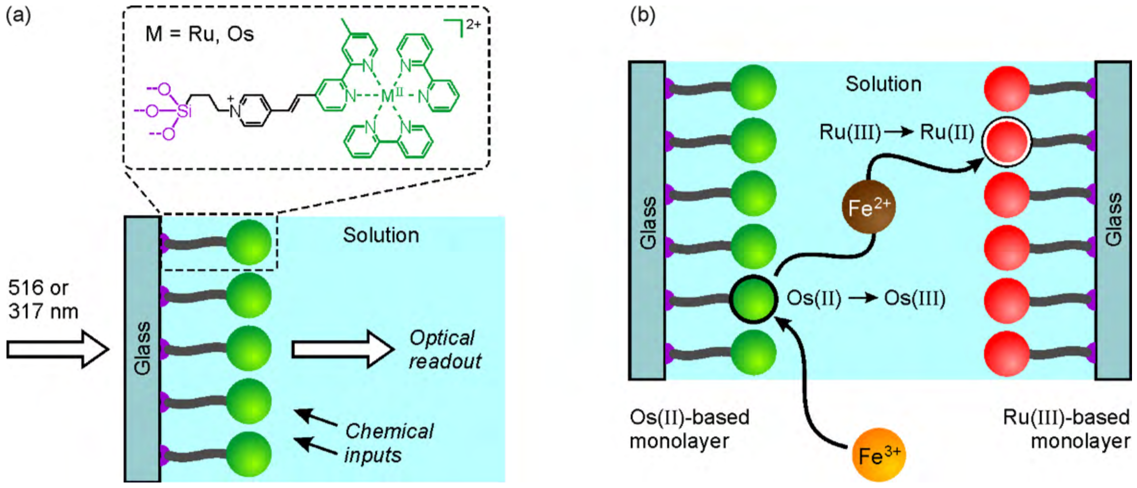

Fig. 14. (a) Structure and operation of the monolayers obtained by covalently linking Ru- or Os-polypyridine complexes to glass surfaces [90–92]. The monolayer is subjected to combinations of chemical inputs in solution and its state is monitored by transmittance measurements, giving rise to input/output relationships corresponding to a variety of binary logic functions. (b) Gate-to-gate chemical communication: upon addition of a Fe^{3+} input to the solution, the Os(II) units of the monolayer are oxidized, thereby releasing a Fe^{2+} output which acts as the input for the Ru(III)-based film immersed in the same solution.

complexes can be switched between the M(II) and M(III) oxidation states using chemical reagents such as Ag^+, $Co(C_5H_5)_2$, NO^+ or Ce^{4+} in a variety of conditions, thus providing a large set of possible inputs. The oxidation state of the surface-bound compounds can be detected easily by measuring the transmittance of the film at ultraviolet and visible wavelengths. Upon combining one, two or three reagents as the chemical inputs, and measuring the optical transmission at selected wavelengths (516 or 317 nm) as the outputs, the osmium-based monolayer is capable of performing the AND, OR, XOR, INH and implication (IMP) operations on two inputs, and even more complex functions on three inputs [92].

In a successive step, the operation of Os(II)- and Ru(III)-based monolayers in the same chemical environment was investigated (Fig. 14). The reaction of the Os(II)-based film with Fe^{3+} ions in acetonitrile results in oxidation of the surface-bound metal centres and the formation of Fe^{2+} ions, which diffuse through the solution and subsequently reduce the Ru(III) centres in the second monolayer. This change can be detected by monitoring the absorbance of the film at 463 nm. Using Ce^{4+} and H_2O as chemical inputs in conjunction with Fe^{3+}, the ensemble mimics the binary operation of a simple combinational circuit [92].

The most interesting aspect of the work, besides the high stability and reversibility of the monolayers, is that the chemical output of one monolayer-based gate can be sent as the input for a downstream gate using the solution as a communication medium. As discussed in Section 3.3, such a result is of high conceptual importance because it is a first step towards the serial connection of different logic devices (cascading).

4. Conclusion

The realization of computing devices with extremely small size, low power consumption and unprecedented performance is a strong motivation for the search of molecule-based bottom-up strategies to information processing. Because of their diverse and valuable physico-chemical properties, metal complexes are attractive candidates to play the role of functional components for the construction of artificial molecular devices capable of elaborating information.

Two philosophically different approaches can be pursued to attain this goal. One is that based on the use of molecules as nanoscale components (e.g., wires and diodes) to construct miniaturized electric circuits [11,93,94]. In such a molecular electronics approach information-processing functions result from circuit architecture rather than from the inherent "intelligent" behaviour of the employed molecules. Many investigations on electrical conductivity and switching properties of single molecules and supermolecules have been performed [95]. However, the mechanisms of charge transport in molecular junctions have not yet been fully understood [95], and much remains to be learned about the means of manipulating, bonding, and ordering them in extended circuit-like structures that can be interfaced with the macroscopic world while maintaining nanoscale addressing [12,93]. Much debate is going on about the promises and achievements of this approach [10,96].

The other approach, inspired by information processing in living organisms, is based on appropriately designed molecular systems that operate in solution by using chemicals, photons or electrons as input/output signals [9,18,54,55,57]. The systems described here belong to this category, sharing with molecular electronic circuits the Boolean numbering system adopted for data representation. However, other choices such as multi-valued [97] and fuzzy logic [98] or variable threshold (neural) mechanisms [99] could also be made.

The molecular electronics approach has the potential advantage of being strictly related to the paradigms of current microelectronics technology [11]. On the other hand, a chemical approach to molecular logic gives the opportunity to implement even complex logic operations with one molecule or supramolecular species. It is difficult, at the present stage, to predict which one of these two strategies will have the greater technological impact, if any. These and other questions regarding the advent of molecular computers (e.g., serial or parallel architectures, solid-state or soft matter) represent one of the big challenges of nanotechnology.

Finally, we would like to emphasize that many logic devices described in this review are based on simple chemical compounds and well documented chemical, electrochemical, photochemical, and photophysical processes taking place in solution, and the methods used to obtain the illustrated results rely on the simultaneous stimulation of large numbers of molecules. From this viewpoint, one could argue that we have simply illustrated some types of chemical reactions.

We have tried to stress, however, the novel conceptual interpretation of the observed processes. Regardless of the possibility of short-term applications as discussed in Section 1.3, we believe that research in this field is interesting for several reasons: (i) at least in principle, some of the described effects can be scaled down to single molecules; (ii) synthetic multistate-multifunctional systems may play the role of models to begin understanding the chemical basis of complex biological processes; (iii) integration of molecular-level devices may be successfully achieved by intermolecular communication based on chemical and light signals, thereby overcoming the difficulty in establishing electrical communication between different molecules; (iv) last, but not least, these studies introduce new concepts in the "old" field of chemistry and stimulate the ingenuity of research workers engaged in the "bottom-up" approach to nanotechnology.

Acknowledgments

We thank Professors V. Balzani and M. Venturi for stimulating discussions. Financial support from the CompReNDe strategic project of the University of Bologna and Fondazione Cassa di Risparmio in Bologna is gratefully acknowledged.

References

[1] R.J. Mitchell, Microprocessor Systems: An Introduction, Macmillan, London, 1995.

[2] J.R. Gregg, Ones and Zeros: Understanding Boolean Algebra, Digital Circuits, and the Logic of Sets, Wiley-IEEE Press, New York, 1998.

[3] D.K. Mynbaev, L.L. Scheiner, Fiber Optic Communication Technology, Prentice Hall, Upper Saddle River, 2001.

[4] J.M. Kahn, K.-P. Ho, Nature 411 (2001) 1007.

[5] J. Dintinger, I. Robel, P.V. Kamat, C. Genet, T.W. Ebbesen, Adv. Mater. 18 (2006) 1645.

[6] D.S. Goodsell, Bionanotechnology—Lessons from Nature, Wiley, Hoboken, 2004.

[7] R.A.L. Jones, Soft Machines: Nanotechnology and Life, Oxford, University Press, New York, 2004.

[8] P. Ball, Nature 406 (2000) 118.

[9] R. Ballardini, P. Ceroni, A. Credi, M.T. Gandolfi, M. Maestri, M. Semeraro, M. Venturi, V. Balzani, Adv. Funct. Mater. 17 (2007) 740.

[10] P. Ball, Nature 445 (2007) 362.

[11] G.F. Cerofolini, Nanoscale Devices—Fabrication, Functionalization and Accessibility from the Macroscopic World, Springer, Berlin, 2009.

[12] J.E. Green, J.W. Choi, A. Boukai, Y. Bunimovich, E. Johnston-Halperin, E. DeIonno, Y. Luo, B.A. Sheriff, K. Xu, Y.S. Shin, H.-R. Tseng, J.F. Stoddart, J.R. Heath, Nature 445 (2007) 414.

[13] G.C. Pimentel, J.A. Coonrod, Opportunities in Chemistry, National Academy of Sciences, National Academy Press, Washington, 1985.

[14] W. Lu, C.M. Lieber, Nat. Mater. 6 (2007) 841.

[15] The International Technology Roadmap for Semiconductors (ITRS), 2007 Edition and 2008 Update, available at www.itrs.net/reports.html.

[16] R. Chau, B. Doyle, S. Datta, J. Kavalieros, K. Zhang, Nat. Mater. 6 (2007) 810.

[17] B.L. Feringa (Ed.), Molecular Switches, 2nd edition, Wiley, New York, 2007.

[18] V. Balzani, A. Credi, M. Venturi, Molecular Devices and Machines—Concepts and Perspectives for the Nanoworld, 2nd edition, Wiley–VCH, Weinheim, 2008.

[19] O. Wenger, Coord. Chem. Rev. 253 (2009) 1439.

[20] F.M. Raymo, Adv. Mater. 14 (2002) 401.

[21] V. Balzani, A. Credi, M. Venturi, ChemPhysChem 3 (2003) 49.

[22] A.P. de Silva, N.D. McClenaghan, Chem. Eur. J. 10 (2004) 574.

[23] D. Gust, T.A. Moore, A.L. Moore, Chem. Commun. (2006) 1169.

[24] A.P. de Silva, S. Uchiyama, Nat. Nanotechnol. 2 (2007) 399.

[25] U. Pischel, Angew. Chem. Int. Ed. 46 (2007) 4026.

[26] K. Szaciłowski, Chem. Rev. 108 (2008) 3481.

[27] N. Wagner, G. Ashkenasy, Chem. Eur. J. 15 (2009) 1765.

[28] J. Andréasson, U. Pischel, Chem. Soc. Rev., 39, in press.

[29] A. Credi, Angew. Chem. Int. Ed. 46 (2007) 5472.

[30] A.P. de Silva, T.P. Vance, M.E.S. West, G.D. Wright, Org. Biomol. Chem. 6 (2008) 2468.

[31] A.P. de Silva, D.Y. James, B.O.F. McKinney, D.A. Pears, S.M. Weir, Nat. Mater. 5 (2006) 787.

[32] G. von Maltzahn, T.J. Harris, J.-H. Park, D.-H. Min, A.J. Schmidt, M.J. Sailor, S.N. Bhatia, J. Am. Chem. Soc. 129 (2007) 6064.

[33] R. Yashin, S. Rudchenko, M.N. Stojanovic, J. Am. Chem. Soc. 129 (2007) 15581.

[34] S. Kou, H.N. Lee, D. van Noort, K.M.K. Swamy, S.H. Kim, J.H. Soh, K.-M. Lee, S.-W. Nam, J. Yoon, S. Park, Angew. Chem. Int. Ed. 47 (2008) 872.

[35] S. Muramatsu, K. Kinbara, H. Taguchi, N. Ishii, T. Aida, J. Am. Chem. Soc. 128 (2006) 3764.

[36] T. Konry, D.R. Walt, J. Am. Chem. Soc. 131 (2009) 13232.

[37] R.J. Amir, M. Popkov, R.A. Lerner, C.F. Barbas III, D. Shabat, Angew. Chem. Int. Ed. 44 (2005) 4378.

[38] Y. Benenson, B. Gil, U. Ben-Dor, R. Adar, E. Shapiro, Nature 429 (2004) 423.

[39] K. Rinaudo, L. Bleris, R. Maddamsetti, S. Subramanian, R. Weiss, Y. Benenson, Nat. Biotechnol. 25 (2007) 795.

[40] V. Balzani, A. Credi, M. Venturi, Proc. Natl. Acad. Sci. U.S.A. 99 (2002) 4814.

[41] E. Ishow, A. Credi, V. Balzani, F. Spadola, L. Mandolini, Chem. Eur. J. 5 (1999) 984.

[42] V. Balzani, M. Clemente-León, A. Credi, J.N. Lowe, J.D. Badjic, J.F. Stoddart, D.J. Williams, Chem. Eur. J. 9 (2003) 5348.

[43] W. Jiang, M. Han, H.-Y. Zhang, Z.-J. Zhang, Y. Liu, Chem. Eur. J. 15 (2009) 9938.

[44] R. Ballardini, V. Balzani, M. Clemente-León, A. Credi, M.T. Gandolfi, E. Ishow, J. Perkins, J.F. Stoddart, H.-R. Tseng, S. Wenger, J. Am. Chem. Soc. 124 (2002) 12786.

[45] B. Ferrer, G. Rogez, A. Credi, R. Ballardini, M.T. Gandolfi, V. Balzani, Y. Liu, H.-R. Tseng, J.F. Stoddart, Proc. Natl. Acad. Sci. U.S.A. 103 (2006) 18411.

[46] G. Rogez, B.F. Ribera, A. Credi, R. Ballardini, M.T. Gandolfi, V. Balzani, Y. Liu, B.H. Northrop, J.F. Stoddart, J. Am. Chem. Soc. 129 (2007) 4633.

[47] C.O. Dietrich-Buchecker, J.-P. Sauvage, Chem. Rev. 87 (1987) 795.

[48] B. Champin, P. Mobian, J.-P. Sauvage, Chem. Soc. Rev. 36 (2007) 358.

[49] U. Létinois-Halbes, D. Hanss, J.M. Beierle, J.-P. Collin, J.-P. Sauvage, Org. Lett. 7 (2005) 5753.

[50] G. Periyasamy, J.-P. Collin, J.-P. Sauvage, R.D. Levine, F. Remacle, Chem. Eur. J. 15 (2009) 1310.

[51] G. Periyasamy, A. Sour, J.-P. Collin, J.-P. Sauvage, F. Remacle, J. Phys. Chem. B 113 (2009) 6219.

[52] A. Aviram, J. Am. Chem. Soc. 110 (1988) 5687.

[53] A.P. de Silva, H.Q.N. Gunaratne, C.P. McCoy, Nature 364 (1993) 42.

[54] V. Balzani, A. Credi, M. Venturi, Chem. Eur. J. 14 (2008) 26.

[55] K. Szaciłowski, Chem. Eur. J. 10 (2004) 2520.

[56] G. Seelig, D. Soloveichik, D.Y. Zhang, E. Winfree, Science 314 (2006) 1585.

[57] A.P. de Silva, Nat. Mater. 4 (2005) 15.

[58] D. Margulies, G. Melman, A. Shanzer, Nat. Mater. 4 (2005) 768.

[59] M. Amelia, M. Baroncini, A. Credi, Angew. Chem. Int. Ed. 47 (2008) 6240.

[60] P. Ceroni, G. Bergamini, V. Balzani, Angew. Chem. Int. Ed. 48 (2009) 8516.

[61] A.P. de Silva, N.D. McClenaghan, Chem. Eur. J. 8 (2002) 4935.

[62] For an example of irreversible reconfiguration in a molecule-based electronic device, see: C.P. Collier, E.W. Wong, M. Behloradsky, F.M. Raymo, J.F. Stoddart, P.J. Kuekes, R.S. Williams, J.R. Heath, Science 285 (1999) 391.

[63] M. de Sousa, B. de Castro, S. Abad, M.A. Miranda, U. Pischel, Chem. Commun. (2006) 2051.

[64] A.P. de Silva, C.M. Dobbin, T.P. Vance, B. Wannalerse, Chem. Commun. (2009) 1386.

[65] A.S. Lukas, P.J. Bushhard, M.R. Wasielewski, J. Am. Chem. Soc. 123 (2001) 2440.

[66] S. Giordani, F.M. Raymo, Proc. Natl. Acad. Sci. U.S.A. 99 (2002) 4941.

[67] O. Kuznetz, H. Salman, N. Shakkour, Y. Eichen, S. Speiser, Chem. Phys. Lett. 451 (2008) 63.

[68] S. Silvi, E.C. Constable, C.E. Housecroft, J.E. Beves, E.L. Dunphy, M. Tomasulo, F.M. Raymo, A. Credi, Chem. Commun. (2009) 1484.

[69] F.M. Raymo, S. Giordani, A.J.P. White, D.J. Williams, J. Org. Chem. 68 (2003) 4158.

[70] E.C. Constable, C.E. Housecroft, A.C. Thompson, P. Passaniti, S. Silvi, M. Maestri, A. Credi, Inorg. Chim. Acta 360 (2007) 1102.

[71] S. Silvi, A. Arduini, A. Pochini, A. Secchi, M. Tomasulo, F.M. Raymo, M. Baroncini, A. Credi, J. Am. Chem. Soc. 129 (2007) 13378.

[72] S. Silvi, E.C. Constable, C.E. Housecroft, J.E. Beves, E.L. Dunphy, M. Tomasulo, F.M. Raymo, A. Credi, Chem. Eur. J. 15 (2009) 178.

[73] J. Andréasson, S.D. Straight, T.A. Moore, A.L. Moore, D. Gust, J. Am. Chem. Soc. 130 (2008) 11122.

[74] C. Giansante, P. Ceroni, M. Venturi, J. Sakamoto, A.D. Schluter, ChemPhysChem 10 (2009) 495.

[75] A. Juris, V. Balzani, F. Barigelletti, S. Campagna, P. Belser, A. von Zelewsky, Coord. Chem. Rev. 84 (1988) 85.

[76] N.E. Tokel, A.J. Bard, J. Am. Chem. Soc. 94 (1972) 2862.

[77] F.M. Raymo, R.J. Alvarado, S. Giordani, M.E. Cejas, J. Am. Chem. Soc. 125 (2003) 2361.

[78] Z.-Q. Guo, W.-H. Zhu, L.-J. Shen, H. Tian, Angew. Chem. Int. Ed. 46 (2007) 5549.

[79] W. Sun, C. Zhou, C.-H. Xu, C.-J. Fang, C. Zhang, Z.-X. Li, C.-H. Yan, Chem. Eur. J. 14 (2008) 6342.

[80] J. Andréasson, S.D. Straight, T.A. Moore, A.L. Moore, D. Gust, Chem. Eur. J. 15 (2009) 3936.

[81] D. Margulies, C.E. Felder, G. Melman, A. Shanzer, J. Am. Chem. Soc. 129 (2007) 347.

[82] D. Margulies, G. Melman, C.E. Felder, R. Arad-Yellin, A. Shanzer, J. Am. Chem. Soc. 126 (2004) 15400.

[83] A. Credi, Nat. Nanotechnol. 3 (2008) 529.

[84] G. Wen, J. Yan, Y. Zhou, D. Zhang, L. Mao, D. Zhu, Chem. Commun. (2006) 3016.

[85] S. Nitahara, N. Terasaki, T. Akiyama, S. Yamada, Thin Solid Films 499 (2006) 354.

[86] M. Biancardo, C. Bignozzi, H. Doyle, G. Redmond, Chem. Commun. (2005) 3918.

[87] K. Szaciłowski, W. Macyk, G. Stochel, J. Am. Chem. Soc. 128 (2006) 4550.

[88] L.F.O. Furtado, A.D.P. Alexiou, L. Gonçalves, H.E. Toma, K. Araki, Angew. Chem. Int. Ed. 45 (2006) 3143.

[89] M. Pita, E. Katz, J. Am. Chem. Soc. 130 (2008) 36.

[90] T. Gupta, M.E. van der Boom, J. Am. Chem. Soc. 129 (2007) 12296.

[91] T. Gupta, M.E. van der Boom, Angew. Chem. Int. Ed. 47 (2008) 2260.

[92] T. Gupta, M.E. van der Boom, Angew. Chem. Int. Ed. 47 (2008) 5322.

[93] R.M. Metzger, Chem. Rec. 4 (2004) 291.

[94] M.A. Reed, T. Lee, Molecular Nanoelectronics, American Scientific Publishers, Stevenson Ranch, 2003.
[95] S.M. Lindsay, M.A. Ratner, Adv. Mater. 19 (2007) 23.
[96] A.H. Flood, J.F. Stoddart, D.W. Steuerman, J.R. Heath, Science 306 (2004) 2055, references therein.
[97] R. Ferreira, P. Remon, U. Pischel, J. Phys. Chem. C 113 (2009) 5805.
[98] P.L. Gentili, Chem. Phys. 336 (2007) 64.
[99] F. Pina, M.J. Melo, M. Maestri, P. Passaniti, V. Balzani, J. Am. Chem. Soc. 122 (2000) 4496.